Langmuir Article

pubs.acs.org/Langmuir

Investigation of the $NaBH_4$-Induced Aggregation of Au Nanoparticles

Zhiqiang Zhang[†,‡] and Yihui Wu*[,†]

[†]*State Key Laboratory of Applied Optics, Changchun Institute of Optics, Fine Mechanics and Physics, Chinese Academy of Sciences, Changchun, Jilin Province 130033, PR China, and* [‡]*Graduate University of the Chinese Academy of Sciences, Beijing 100049, PR China*

Received November 21, 2009. Revised Manuscript Received May 2, 2010

Colloidal Au nanoparticles (AuNPs) with a diameter of 17 nm were prepared by the reduction of $HAuCl_4$ with citrate trisodium. The addition of $NaBH_4$ to the prepared citrate-stabilized AuNP solutions not only induced a blue shift in the surface plasmon resonance peak (λ_{max}) because of the increased number of electrons in the NPs injected by $NaBH_4$ but also affected the stability of citrate adsorbed on AuNPs. The zeta potential of AuNPs after the addition of 6 mM $NaBH_4$ decreased (67%) but was restored (88%) after the discharge of the injected electrons. The effect of $NaBH_4$ treatment on the stability of citrate ions on AuNPs was investigated by X-ray photoelectron spectroscopy (XPS). The XPS data showed that citrate ions partially desorbed from the surfaces of AuNPs (67%) after $NaBH_4$ treatment but readsorbed onto the AuNPs (80%) after the discharge of the NPs; this result agrees well with the zeta potential data. The partial removal of citrate ions from AuNPs results in an anisotropic charge distribution around the AuNPs. By increasing the amount of $NaBH_4$ and the electrolyte concentration of the solution, non-close-packed aggregates of AuNPs can be formed, from monomers to small aggregates containing a few AuNPs and 3D network aggregates.

Introduction

Unique assemblies composed of nanoparticles (NPs) can provide distinct electronic,[1] chemical,[2] and optical[3] properties relative to individual NPs and have a wide range of applications in electronics, plasmonics, sensors, and surface-enhanced Raman scattering (SERS).[4] All of these potential applications of the assemblies depend on the controllable assembly of NPs into desired architectures. One key in the self-assembly of NPs is to control the thermodynamic balance of interactions between NPs, which includes long-range electrostatic repulsion, short-range van der Waals attraction, and other short-range interactions.[5] More importantly,the anisotropic interaction between NPs is necessary to form more advanced nanostructures such as low-dimensional anisotropic nanostructures and more complex assemblies in a designable way.[6] The anisotropic interaction can originate from intrinsic magnetic or electric dipoles in NPs, by which 1D[7] and 2D[8] assemblies have been formed in solution. In contrast, for those metallic NPs with no intrinsic dipolar interactions, an anisotropic interaction can be obtained through tuning the isotropic electrostatic interaction into an anisotropic one by partially replacing the stabilizer of NPs with other chemicals such as CTAB,[9,10] MEA,[11] and dithoil[12] to produce an anisotropic surface charge distribution and eventually induce multidimensional assemblies of AuNPs, where the partial modification of the NPs is due to the anisotropic surface chemistry of NPs.[13] Besides, an anisotropic surface charge distribution can be obtained by partial neutralization of the surface charge with counterionic species.[14] Another way to produce anisotropy is to partially remove the stabilizer on the NPs. For example, by removing excess stabilizer in solution and redispersing it in pure water, linear assemblies can be formed after several hours or days.[15] However, a long time is usually necessary in this method for the removal of stabilizing molecules from the surfaces of the NPs because of its slow desorption kinetics.

Treating the AuNPs with $NaBH_4$ by utilizing electrons transfer into the NPs is the most direct way to change their optical and chemical properties.[16,17] By electron injection into AuNPs, the property of the AuNPs may be greatly changed because of the modification of the electron configuration of the Au atom under excess free electrons. However, to the best of our knowledge, the

*To whom correspondence should be addressed. Tel: +86-0431-86176915. Fax: +86-0431-85690271. E-mail: yihuiwu@ciomp.ac.cn.

(1) Andres, R. P.; Bielefeld, J. D.; Henderson, J. I.; Janes, D. B.; Kolagunta, V. R.; Kubiak, C. P.; Mahoney, W. J.; Osifchin, R. G. *Science* **1996**, *273*, 1690.
(2) Murugadoss, A.; Chattopadhyay, A. *J. Phys. Chem. C* **2008**, *112*, 11265.
(3) Wessels, J. M.; Nothofer, H.-G.; Ford, W. E.; Wrochem, F. von; Scholz, F.; Vossmeyer, T.; Schroedter, A.; Veller, H.; Yasuda, A. *J. Am. Chem. Soc.* **2004**, *126*, 3349.
(4) (a) Fendler, J. H. *Chem. Mater.* **2001**, *13*, 3196. (b) Maier, S. A.; Brongersma, M. L.; Kik, P. G.; Meltzer, S.; Requicha, A. A. G.; Atwater, H. A. *Adv. Mater.* **2001**, *13*, 1501. (c) Krasteva, N.; Besnard, I.; Guse, B.; Bauer, R. E.; Müllen, K.; Yasuda, A.; Vossmeyer, T. *Nano Lett.* **2002**, *2*, 551–555. (d) Tessier, P. M.; Velev, O. D.; Kalambur, A. T.; Rabolt, J. F.; Lenhoff, A. M.; Kaler, E. W. *J. Am. Chem. Soc.* **2000**, *122*, 9554. (e) Shipway, A. N.; Katz, E.; Willner, I. *ChemPhysChem* **2000**, *1*, 18.
(5) (a) Min, Y.; Akulut, M.; Kristairsen, K.; Golan, Y.; Israelachvili, J. *Nat. Mater.* **2008**, *7*, 527. (b) Bishop, K. J. M.; Wilmer, C. E.; Soh, S.; Grzybowski, B. A. *Small* **2009**, *5*, 1600. (c) Lyklema, J. Fundamentals of Interface and Colloid Science. In *Particulate Colloids*; Elsevier/Academic Press: Amsterdam, 2005; Vol. *IV*.
(6) (a) Glotzer, S. C.; Solomon, M. J. *Nat. Mater.* **2007**, *6*, 557. (b) Glotzer, S. C. *Science* **2004**, *306*, 419.
(7) (a) Thomas, J. R. *J. Appl. Phys.* **1966**, *37*, 2914. (b) Tang, Z.; Kotov, N.; Giersig, M. *Science* **2002**, *297*, 237. (c) Wang, X.; Li, G.; Chen, T.; Yang, M.; Zhang, Z.; Wu, T.; Chen, H. *Nano Lett.* **2008**, *8*, 2643. (d) Roca, M.; Pandya, N. H.; Nath, S.; Haes, A. J. *Langmuir* **2010**, *26*, 2035.
(8) (a) Wiedwald, U.; Spasova, M.; Farle, M.; Hilgendorff, M.; Giersig, M. *J. Vac. Sci. Technol., A* **2001**, *19*, 1773. (b) Tang, Z.; Zhang, Z.; Wang, Y.; Glotzer, S. C.; Kotov, N. *Science* **2006**, *314*, 274.
(9) Yang, Y.; Matsubara, S.; Nogami, M.; Shi, J.; Huang, W. *Nanotechnology* **2006**, *17*, 2821.
(10) Ji, Q.; Acharya, S.; Hill, J. P.; Richards, G. J.; Ariga, K. *Adv. Mater.* **2008**, *20*, 4027.
(11) Lin, S.; Li, M.; Dujardin, E.; Girard, C.; Mann, S. *Adv. Mater.* **2005**, *17*, 2553.
(12) Hussain, I.; Brust, M.; Barauskas, J.; Cooper, A. I. *Langmuir* **2009**, *25*, 1934.
(13) Zhang, H.; Fung, K. H.; Hartmann, J.; Chan, C. T.; Wang, D. *J. Phys. Chem. C* **2008**, *112*, 16830.
(14) Shipway, A. N.; Lahav, M.; Gabai, R.; Willner, I. *Langmuir* **2000**, *16*, 8789.
(15) Richardi, J. *J. Chem. Phys.* **2009**, *130*, 044701.
(16) Tunc, I.; Guvenc, H. O.; Sezen, H.; Suzer, S.; Correa-Duarte, M. A.; Liz-Marzán, L. M. *J. Nanosci. Nanotechnol.* **2008**, *8*, 3003.
(17) Panigrahi, S.; Basu, S.; Praharaj, S.; Pande, S.; Jana, S.; Pal, A.; Ghosh, S. K.; Pal, T. *J. Phys. Chem. C* **2007**, *111*, 4596.

effects of $NaBH_4$ treatment on other properties of colloidal AuNPs, such as the electrical double layer and the interactions between the NPs, are ignored in previous studies.

Here, we studied the effect of $NaBH_4$ treatment on the stability of colloidal AuNPs. Citrate-stabilized AuNPs (17 nm in diameter) were used as a model system. We found that AuNPs formed non-close-packed aggregates and 3D network aggregates depending on the amount of $NaBH_4$ and the electrolyte concentration of the solution. The aggregation of AuNPs was attributed to the decrease in surface potential that resulted from electron injection into the AuNPs by $NaBH_4$. The reason that $NaBH_4$ induced a decrease in surface potential was investigated by zeta potential and X-ray photoelectron spectroscopy. The data showed that citrate ions were partially removed from the surfaces of AuNPs after $NaBH_4$ addition but that they adsorbed again after the discharge of the AuNPs. The mechanism of $NaBH_4$-induced anisotropic aggregation of AuNPs was also discussed.

Experimental Section

Materials. Sodium borohydride ($NaBH_4$, ≥98%) and (3-aminopropyl)triethoxysilane (APTES, 99%) were purchased from Aldrich. Hydrogen tetrachloroaurate ($HAuCl_4 \cdot 4H_2O$, >99.9%), silver nitrate ($AgNO_3$, >99.9%), and trisodium citrate ($C_6H_5O_7Na_3 \cdot 2H_2O$, ≥99.0%) were purchased from Beijing Chemical Reagents (Beijing, PR China) and used without further purification. Milli-Q water (18.2 $M\Omega \cdot cm^{-1}$) was used for all experiments. All other reagents were analytical grade.

Synthesis of Gold and Silver Nanoparticles. An aqueous suspension of citrate-stabilized gold nanoparticles (with a size of 17 nm) was prepared by the reduction of $HAuCl_4$ with citrate.[18] Briefly, 200 mL of 0.01% (w/v) $HAuCl_4$ solution was heated to boiling under vigorous string with refluxing, and 1 min later, 8 mL of 1% (w/v) sodium citrate was rapidly added to the boiling solution and the mixture was allowed to boil for 20 min. Then, the prepared gold colloids were cooled to room temperature with constant stirring and stored at 4 °C in a dark bottle. An aqueous suspension of citrate-stabilized silver nanoparticles (AgNPs) was prepared by the reduction of $AgNO_3$ with $NaBH_4$ in the presence of citrate ions.[19] Briefly, an aqueous solution of $NaBH_4$ (3 mL, 10 mM) was added to a 100 mL solution of $AgNO_3$ (0.25 mM) and trisodium citrate (0.25 mM). The mixture was stirred for 30 min. The prepared silver colloids were then left undisturbed overnight at room temperature before use. All glassware was rigorously cleaned in aqua regia solution (3:1 HCl/HNO_3) and then rinsed thoroughly with Milli-Q H_2O before use.

Preparation of APTES-Derivatized Substrates. According to a previous method,[20] the silicon slides were cleaned in piranha solution (7:3 H_2SO_4/30% H_2O_2) at 120 °C for 20 min, rinsed extensively with distilled water, and dried in a pure N_2 flow. ***Caution!*** *Piranha solution is very corrosive and must be handled with extreme care*. After being rinsed with methanol for 5 min, the substrates were immersed in 5% (v/v) APTES in methanol for 1 h and rinsed five times in methanol by inversion for 10 min, followed by DI water to hydrolyze residual ethoxy functionalities for 30 min. Thereafter, the slides were then dried in a pure N_2 flow and at 120 °C for 1 h to promote cross-linking of the silanes. The APTES-derivatized silicon slides (noted as SiO_2/APTES) were stored in a desiccator for further use.

$NaBH_4$ Treatment of Gold and Silver Nanoparticles. To study the effect of the concentration of $NaBH_4$ on AuNP aggregation, different amounts of ice-cold 0.2 M $NaBH_4$ were added to a quartz cuvette containing 0.5 mL of gold sol, and the mixture was rapidly mixed for 3 s. To study the effect of the ionic strength of $NaBH_4$ on the aggregation of AuNPs for a constant amount of $NaBH_4$, 15 μL of ice-cold 0.2 M $NaBH_4$ was added and mixed, followed by the addition of different amounts of 0.2 M NaCl (pH 10.5). To study the effect of $NaBH_4$ on citrate ions on AuNP, the silicon slides functionalized with APTES were immersed in gold sol for 12 h to form a submonolayer of AuNP, followed by rinsing with Milli-Q water to remove unbound AuNPs. Then, the AuNP monolayer was immersed in a solution of $NaBH_4$ (0.23 M) for 20 min, followed by rinsing with Milli-Q water and drying in air. To study the effect of the concentration of $NaBH_4$ on AgNP aggregation, 30 μL of 0.2 M $NaBH_4$ was added to 0.5 mL of silver sol. The cuvettes were sealed with Parafilm after the addition of $NaBH_4$ or NaCl to prevent evaporation. The APTES/SiO_2 substrates were used to characterize the morphologies of aggregates of AuNPs and AgNPs. Briefly, the APTES/SiO_2 slides were immersed in the solution of aggregates for 1 to 2 h, followed by rinsing with Milli-Q water and drying in air. By this method, AuNP aggregates would be bound to the APTES/SiO_2 surface through electrostatic attraction, and this would avoid the effect of drying on aggregate morphology. In this study, suspensions of AuNPs and AgNPs were used without dilution for all experiments. The concentration of gold NPs was calculated to be ~1.86 nM (1.12×10^9 NPs/mL) by assuming that all added Au^{3+} ions were reduced to Au^0 atoms by citrate in solution and that the formed AuNPs had an average diameter of 17 nm.

Characterization Methods. All UV−vis extinction spectra were measured using a Perkin-Elmer Lambda 850 UV/vis spectrophotometer. The morphologies of formed assemblies of NPs were characterized by a Hitachi S-4800 field-emission scanning electron microscope (FE-SEM). X-ray photoelectron spectroscopy (XPS) was conducted with a VG ESCALAB MKII spectrometer (VG Scientific, U.K.) by employing a monochromatic Al Kα source ($h\nu$ = 1486.6 eV). All binding energies were referenced to the C 1s neutral carbon peak at 284.6 eV. For XPS characterization, 15 μL of 0.2 M $NaBH_4$ was added to 0.5 mL of AuNPs in a 1.5 mL reagent bottle and mixed. After 10 min or 5 days, the AuNPs were collected by centrifuging twice at 9000 rpm, discarding the supernatant, and redispersing the AuNPs in 10 μL of pure water. For a contrast sample, 0.5 mL of AuNPs was centrifuged twice at 9000 rpm/min and redispersed in 10 μL of pure water. These obtained precipitates were dropped onto silicon slides and dried in air. The zeta potential of the AuNPs was measured on a Malvern Zetasizer Nano-ZS90 (Malvern Instruments Ltd., U.K.) at 25.0 ± 0.1 °C.

Theory of the Stability of Colloidal NPs.[21,22] Generally, the stability of colloidal particles in an aqueous solution is described by classical DLVO (Derjaguin−Landau−Vervey−Overbeek) theory. For monodisperse spherical NPs, the total interaction potential, V_T, is the sum of the electrostatic repulsive potential (V_{elec}) and the van der Waals attractive potential (V_{vdW})[23,24]

$$V_T(r) = V_{elec}(r) + V_{vdW}(r) \quad (1)$$

$$V_{elec}(r) = 2\pi\varepsilon_s\varepsilon_0 a\psi_0^2 \ln[1+\exp(-\kappa H)] \quad (\kappa a > 5) \quad (2)$$

$$V_{elec}(r) = 4\pi\varepsilon_s\varepsilon_0 a^2 Y^2 \left(\frac{k_B T}{e}\right)^2 \frac{\exp(-\kappa H)}{r} \quad (\kappa a < 5) \quad (3)$$

(18) Frens, G. *Nat. Phys. Sci.* **1973**, *241*, 20.
(19) Doty, R. C.; Tshikhudo, T. R.; Brust, M.; Fernig, D. G. *Chem. Mater.* **2005**, *17*, 4630.
(20) Howarter, J. A.; Youngblood, J. P. *Langmuir* **2006**, *22*, 11142.
(21) Verwey, E. J. W.; Overbeek, J. Th. G. *Theory of the Stability of Lyophobic Colloids*; Elsevier: New York, 1948.
(22) Israelachvili, J. N. *Intermolecular and Surface Forces*; Academic Press: London, 1992.
(23) Kim, T.; Lee, K.; Gong, M.; Joo, S. W. *Langmuir* **2005**, *21*, 9524.
(24) Hunter, R. J. *Foundations of Colloid Science*; Clarendon Press: Oxford, U.K, 1987; Vol. *1*, Chapter 7.

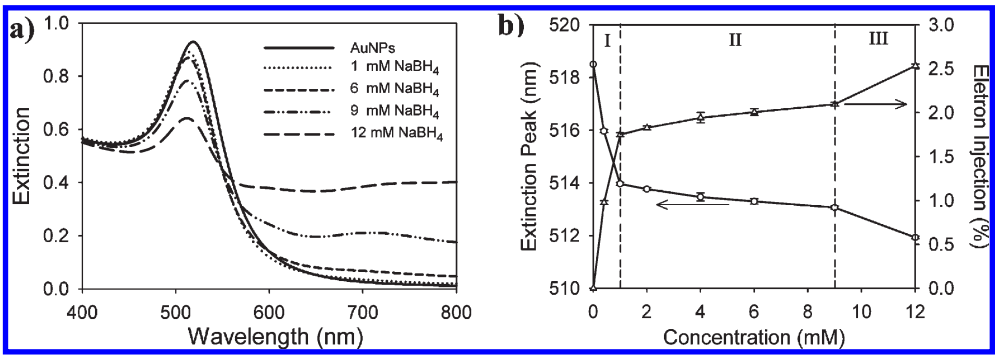

Figure 1. (a) UV/vis extinction spectra of citrate-stabilized AuNP (particle size 17 nm) solutions recorded 3 min after the addition of 1, 6, 9, and 12 mM $NaBH_4$. (b) Shift of the extinction peak (λ_{max}) of AuNP solutions after the addition of different amounts of $NaBH_4$ and the corresponding calculated rate of electron injection.

$$Y = \frac{8\tanh(e\psi_0/4k_BT)}{1+\left[1-\frac{2\kappa a+1}{(\kappa a+1)^2}\tanh^2(e\psi_0/4k_BT)\right]^{1/2}} \quad (4)$$

$$\kappa = \left[\frac{1000e^2N_A(2I)}{\varepsilon_s\varepsilon_0k_BT}\right]^{1/2} \quad (5)$$

$$V_{vdW}(r) = -\frac{A_H}{6}\left[\frac{2}{R^2-4}+\frac{2}{R^2}+\ln\frac{R^2-4}{R^2}\right] \quad (6)$$

where r is the center-to-center distance of neighboring NPs of radius a ($R = r/a$), H is the distance of closet approach ($r = H + 2a$), ε_s is the relative dielectric constant of the solvent (about 80 for water), ε_0 is the dielectric constant of vacuum, Ψ_0 is the surface potential of NPs, κ is the inverse Debye length ($1/\kappa = 0.304/[NaCl]^{1/2}$ nm for 1:1 electrolytes), and A_H is the Hamaker constant of the particles (2.5×10^{-19} J). The value of the surface potential (Ψ_0) is related to the amount of surface charge that could be obtained in several ways,[25] the preferential adsorption of ions, the dissociation of surface groups, isomorphic substitution, the adsorption of polyelectrolytes, and the accumulation of electrons. For citrated-stabilized NPs, the surface negative charges are generated from deprotonated −COOH groups in citrate ions.

Results and Discussion

Aggregation of Citrate-Stabilized AuNPs Induced by $NaBH_4$. It is known that the spectrum of localized surface plasmon resonance (LSPR)[26] of nanoparticles is influenced by the size, shape, interparticle interactions, free electron density, and surrounding medium.[27] Therefore, it is an efficient tool for monitoring the electron injection and aggregation of NPs.

As expected,[29] the extinction maximum peak (λ_{max}) of AuNPs showed a blue shift after the addition of $NaBH_4$ as a result of an increased number of free electrons (Figure 1a). The relationship between the shift in the extinction maximum wavelength ($\Delta\lambda$) and the change in the electron density (ΔN) is given by Mulvaney.[28]

$$\frac{\Delta N}{2N} = -\frac{\Delta\lambda}{\lambda_0} \quad (7)$$

Here, N is the electron density of the metal, and λ_0 is the position of the surface plasmon band for the case of no electron injection. The shift of λ_{max} and the calculated rate of electron injection according to eq 7 were crudely divided into three regions, as shown in Figure 1b. In the first region (0 to 1 mM), the λ_{max} shifted 4.5 nm toward shorter wavelengths and the slope was 4.5 nm/mM. However, there was only a 1 nm shift in the λ_{max} in the second region (1−9 mM), and the slope decreased to 0.125 nm/mM, which seems that the electron injection into the AuNPs by $NaBH_4$ almost reached saturation. In the third region (9−12 mM), the λ_{max} showed a 1.2 nm shift and the slope increased to 0.4 nm/mM, which indicates enhanced electron injection. It should be pointed out that the blue shift of λ_{max} of NPs could also result from the transverse plasmon band of 1D chains.[30] Therefore, the calculated rate of electron injection may not be precise when chainlike aggregates are formed.

Besides the blue shift in λ_{max}, extinction bands above 600 nm showed different shapes with increasing concentration of $NaBH_4$. Different shapes in these extinction spectra at longer wavelengths indicated different extents of AuNP aggregation. At low $NaBH_4$ concentration (6 mM), a flattened extinction band above 600 nm was slightly higher than that before the addition of $NaBH_4$. This weak flattened band could not be simply regarded as the formation of small aggregates. It may be partially due to some unknown effects induced by excess injected electrons because this kind of flattened band could also be identified in the extinction band induced by a much lower concentration of $NaBH_4$ (1 mM). And this weak flattened band may always exist as a background in the extinction band induced by ahigher concentration of $NaBH_4$. A weak broaded extinction peak at 710 nm with increased extinction showed up when the concentration of $NaBH_4$ was 9 mM, which means that more large aggregates formed compared to the number induced by 6 mM $NaBH_4$. This peak shifted to 730 nm and became more broadened for the 12 mM $NaBH_4$ treatment, and the extinction band above 560 nm became nearly flat. Such a transition could be regarded as further aggregation based on aggregates induced by 9 mM $NaBH_4$.

The shapes of the optical spectra of AuNPs treated with $NaBH_4$ for 1 h were not changed significantly, except for a slight increase in the extinction band above 600 nm and the return of the

(25) Hiemenz, P. C.; Rajagopalan, R. *Principles of Colloid and Surface Chemistry*, 3rd ed.; Marcel Dekker: New York, 1997; Chapters 11 and 12.
(26) Willets, K. A.; Van Duyne, R. P. *Ann. Rev. Phys. Chem.* **2007**, *58*, 267.
(27) Ghosh, S. K.; Pal, T. *Chem. Rev.* **2007**, *107*, 4797.
(28) Mulvaney, P.; Pérez-Juste, J.; Giersig, M.; Liz-Marzán, L. M.; Pecharromán, C. *Plasmonics* **2006**, *1*, 61.
(29) Mulvaney, P. *Langmuir* **1996**, *12*, 788.
(30) (a) Sawitowski, T.; Miquel, Y.; Heilmann, A.; Schmid, G. *Adv. Funct. Mater.* **2001**, *11*, 435. (b) Harris, N.; Arnold, M. D.; Blaber, M. G.; Ford, M. J. *J. Phys. Chem. C* **2009**, *113*, 2784.

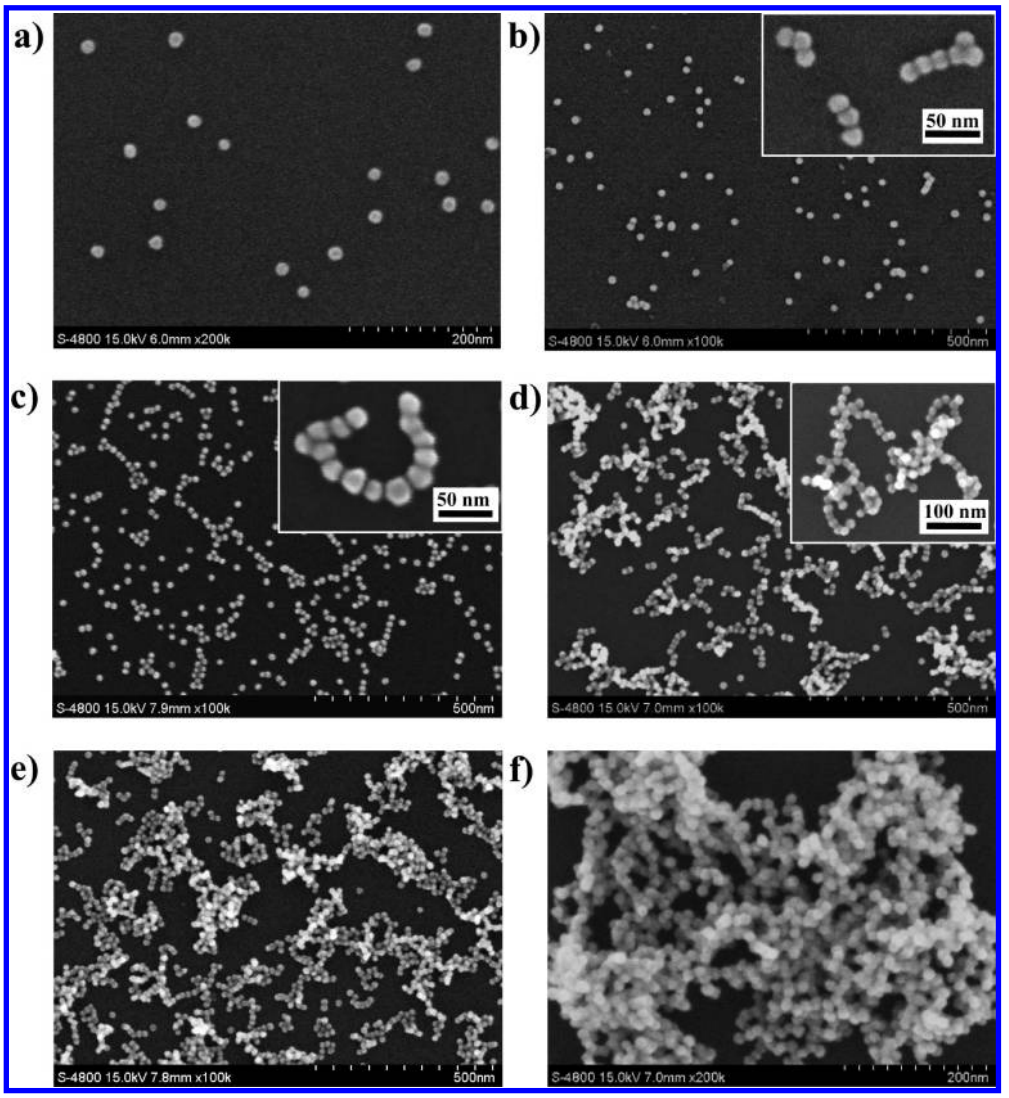

Figure 2. SEM images of AuNP aggregates formed after the addition of different amounts of $NaBH_4$: (a) 0, (b) 6, (c) 7.5, (d) 9, (e) 10, and (f) 12 mM.

position of λ_{max} induced by 1 mM $NaBH_4$ (Figure S1), which indicated that the aggregation of AuNPs was almost complete in the first few minutes after the addition of $NaBH_4$. Figure 2 shows typical scanning electron microscopy (SEM) images of different degrees of AuNP aggregation. It can be clearly seen that more non-close-packed aggregates formed as the concentration of $NaBH_4$ increased from monomers to dimers, trimers, irregular chainlike aggregates, and 3D network aggregates. Accordingly, the extinction band between 600 and 800 nm may be approximately regarded as a collective longitudinal plasmon band of gold nanorods with various aspect ratios but all having the same transverse diameter of ~17 nm. Specifically, the flat band should arise from increased effects of scattering, phase retardation, and higher multipoles because the size of assemblies is comparable to the wavelength, which cannot satisfy the quasi-static approximation.31 The fusion of AuNP aggregates induced by a high concentration of $NaBH_4$ (≥9 mM) may be due to the excess electrons in AuNPs. Chattopadhyay et al.[2] reported similar result.

It is shown that 6 mM $NaBH_4$ caused a few small AuNP aggregates to form (Figure 2), which can be treated as the critical point where aggregation begins. The addition of NaCl into preactivated AuNP solutions resulted in a noticeable extinction band between 600 and 800 nm, and this band became more significant as the amount of NaCl increased (Figure 3a). SEM images (Figures 2b and 3b−d) clearly demonstrated that longer irregular chainlike aggregates and 3D non-close-packed aggregates were formed as the ionic strength increased. The optical spectra did not change after 24 h and were found to stay stable for at least 3 days (Figure S2). This indicated that the aggregates that formed in solution were stable. It is worth noting that the fusion of aggregates became more apparent as the amount of NaCl increased. According to the DLVO theory, increasing the ionic strength can decrease the electrostatic repulsion as well as the thickness of the electrical double layer of colloidal NPs. We also found that addition of NaF or NaOH to the preactivated AuNP solutions had an effect that was similar to that of NaCl (Figure S3). Therefore, we conclude that the aggregation of AuNPs could be finely controlled by tuning the ionic strength of the solution.

In contrast, the shape of the optical spectrum of AuNPs after the addition of 12 mM NaCl did not change, except for a decrease in the height of the extinction peak due to the dilution effect of adding NaCl, which means that the electrolyte concentration of 12 mM does not affect the stability of the AuNPs (Figure 4a). The

(31) Kreibig, U.; Vollmer, M. *Optical Properties of Metal Clusters*; Springer: Berlin, 1995.

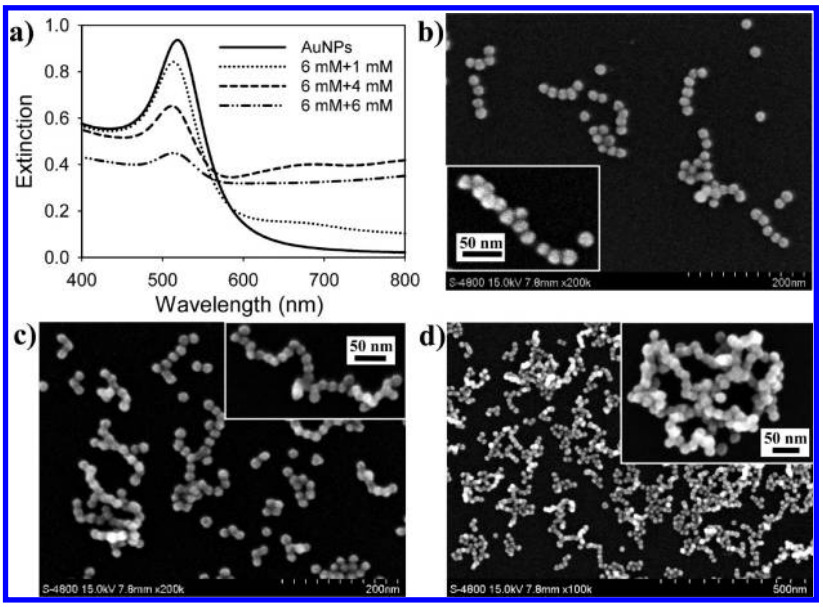

Figure 3. (a) UV/vis extinction spectra of AuNP solutions pretreated with 6 mM $NaBH_4$ after the addition of 1, 4, and 6 mM NaCl. (b−d) SEM images of AuNP self-assemblies formed in the presence of additional $NaBH_4$ and NaCl: (b) 6 + 1 mM, (c) 6 + 4 mM, and (d) 6 + 6 mM. The optical spectra were recorded 1 h after the addition of NaCl. The corresponding high-magnification SEM images are shown in the insets.

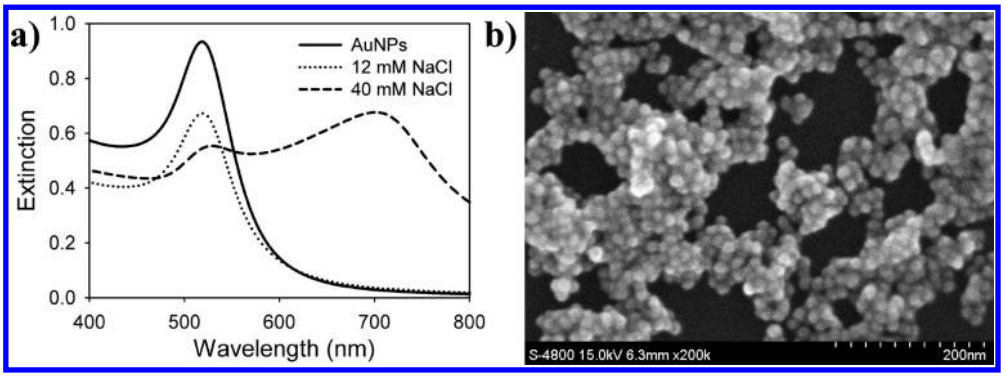

Figure 4. (a) UV/vis extinction spectra of AuNP solutions before and after the addition of 12 and 40 mM NaCl. The optical spectra were recorded 5 min after the addition of NaCl. (b) SEM image of AuNP aggregation induced by 40 mM NaCl.

addition of 40 mM NaCl induced a red shift of λ_{max} in the AuNPs and resulted in a second apparent extinction peak at about 700 nm, which indicated the large extent of AuNP aggregation. The corresponding SEM image showed that fused close-packed AuNP aggregates were formed (Figure 4b). The different morphologies of AuNP aggregates and the different shapes of the spectra induced by 40 mM NaCl (Figure 4b) and 12 mM $NaBH_4$ (Figure 2f) indicated their distinct mechanisms of aggregation.

Zeta Potential Measurement. The zeta potential ζ is related to the surface charge (q) of the particle and the nature and composition of the surrounding medium (pH, κ) in which the particle is dispersed,[32] which can be described as follows:[25]

$$\zeta = \frac{q}{4\pi\varepsilon a}\exp[-\kappa a] \qquad (8)$$

More importantly, the surface charge depends on the degree of ionization of COOH groups of citrates on AuNPs and hence the pH of the suspension. It is well known that $NaBH_4$(aq) is alkaline because it reacts slowly with water ultimately to form strongly basic metaborate ions and generate hydrogen.[33] Here, one problem is that the addition of $NaBH_4$ to the AuNP solution could alter the pH of the mixture and that this pH is time-dependent because $NaBH_4$ hydrolysis must reach equilibrium. Table S1 shows the pH of AuNP solutions after the addition of various amounts of $NaBH_4$ over 5 days. We found that the pH values were not changed after 24 h. The pH of as-prepared AuNPs was 5.2, and the maximum pH after the addition of $NaBH_4$ was up to 9.7 (12 mM after 5 days). To know the effect of pH values on zeta potentials, the pH of as-prepared AuNP solutions was adjusted from 6.5 to 10.0. However, the zeta potentials of AuNP solutions (pH 5.2−10) had almost the same values with increasing pH (Figure S4). Similar results were obtained by Franzen et al.[34] for zeta potentials of citrate-stabilized AuNP suspensions at pH 5−12. No further change in the zeta potential at above pH 5.0 could be due to the complete ionization of COOH groups because the gold colloids have an isoelectric point of about 2.[35]

Therefore, the greatly decreasing ζ value 10 min after the addition of 3 mM (46%) and 6 mM (49%) $NaBH_4$ as shown in

(32) McFadyen, P.; Fairhurst, D. Zeta Potential of Nanoceramic Materials: Measurement and Interpretation. In *NanoCeramics*; Freer, R., Ed.; British Ceramic Proceedings No. 51; Institute of Materials: London, 1993.

(33) Schlesinger, H. I.; Brown, H. C.; Finholt, A. E.; Gilbreath, J. R.; Hoekstra, H. R.; Hyde, E. K. *J. Am. Chem. Soc.* **1953**, *7*, 215.

(34) Brewer, S. H.; Glomm, W. R.; Johnson, M. C.; Knag, M. K.; Franzen, S. *Langmuir* **2005**, *21*, 9303.

(35) Thompson, D.; Collins, I. J. *Colloid Interface Sci.* **1992**, *152*, 197.

Table 1. Zeta Potential of Citrate-Stabilized AuNPs after the Addition of Various Concentrations of NaCl and $NaBH_4$ within 5 Days

		NaCl (mV)			$NaBH_4$ (mV)[a]		
time	control	3 mM	6 mM	12 mM	0.4 mM	3 mM	6 mM
10 min (A)	-43.8 ± 5.4	-38.3 ± 4.76	-38.1 ± 3.86	-36.1 ± 5.72	-40.5 ± 5.43	-23.8 ± 10.3	-22.2 ± 12.4
24 h	-44.6 ± 6.5	-37.6 ± 6.71	-35.4 ± 5.63	-32.3 ± 5.82	-39.9 ± 6.72	-35.6 ± 8.17	-29.1 ± 8.05
5 days (B)	-42.3 ± 5.8				-40.8 ± 7.34	-38.1 ± 7.09	-33.6 ± 7.48
A purified (C)	-61.5 ± 6.28	-60.4 ± 8.42	-61.3 ± 8.75			-47.3 ± 9.85	-44.7 ± 8.2
C 24 h (D)	-41.1 ± 13	-44.3 ± 14	-49.9 ± 24.3			-41.3 ± 10.8	-42.2 ± 9.46

[a] In the 10 min measurement after the addition of 3 and 6 mM $NaBH_4$, many small bubbles appeared on the surfaces of the two electrodes of the detection cell within about 3 min after measuring the zeta potential. However, no air bubbles were found during 24 h of measurement. These bubbles were probably hydrogen and were generated during the loading of high voltage between the two electrodes in the presence of excess $NaBH_4$. No bubbles were found in purified AuNP samples.

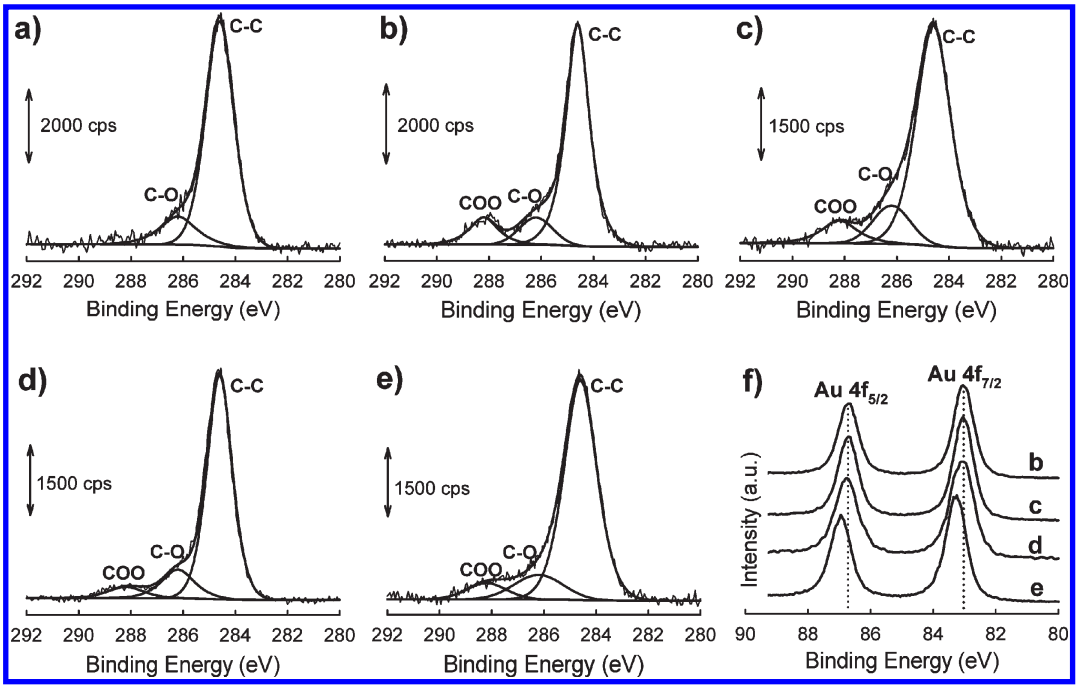

Figure 5. Deconvolved XPS spectra of the C 1s region for (a) the silicon substrate, concentrated AuNPs (b) before and (c) after purification with H_2O, and purified AuNPs via 6 mM $NaBH_4$ treatment after (d) 10 min and (e) 5 days. (f) XPS spectra of the Au 4f region for samples b−e.

Table 1 should be due to the decrease in the surface charge (or Ψ_0) or the increased ionic strength of the solution. However, the ζ value decreased only a little after the addition of 3 mM (13%) and 6 mM (13%) NaCl. This significant difference in the decreasing ζ value for the same amounts of NaCl and $NaBH_4$ means that the $NaBH_4$ treatment induced an additional decrease in the zeta potential. According to eq 8, the ζ value is proportional to the amount of surface charge q if the concentration of added electrolyte remains the same. For a crude calculation, the decreases in AuNP surface charge 10 min after treatment with 3 and 6 mM $NaBH_4$ are 38 and 42% relative to 3 and 6 mM NaCl after 10 min, respectively. Additionally, the increase of these two ζ values after 5 days implies the restoration of AuNP surface charge: 99 and 88% relative to 3 and 6 mM NaCl after 10 min, respectively. Here, we used the ζ values of NaCl-treated AuNPs at 10 min as the reference for "10 min" and "5 days" so as to compare the restoration of the surface charge after the addition of $NaBH_4$ within 5 days.

To determine any possible effects of excess $NaBH_4$ in solution (air bubbles) on the zeta potential measurement, AuNPs were purified by centrifugation and redispersion in pure water after the addition of $NaBH_4$. Care was taken to ensure that the supernatants were completely removed without disturbing the concentrated AuNPs. In a pure water environment, the zeta potential of all purified AuNP samples greatly increased because of the very lower κ value of pure water. The decreases in the rates of change of the zeta potentials (or surface charges) of AuNPs treated with 3 and 6 mM $NaBH_4$ measured in pure water were 33 and 37% relative to that of the control sample, respectively. It is worth noting that the two decreased rates of zeta potential change in pure water are both 5% lower than that before purification. This 5% difference between the decreased rate of ζ change before and after purification may due to the effect of bubbles generated by excess $NaBH_4$ in solution.

By contrast, the zeta potentials of AuNPs purified in the presence of 3 and 6 mM NaCl were the same as the control value, which means that increased ionic strength due to the addition of NaCl or $NaBH_4$ does not affect the zeta potential 10 min after centrifugation. However, the zeta potentials of the control, 3 and 6 mM NaCl, decreased greatly after 24 h and the standard deviations (SD) of the zeta potentials were increased with increasing ionic strength of solution. This means that the AuNPs were not stable in pure water because citrate ions desorbed from AuNPs. For $NaBH_4$-treated samples, the value of ζ showed a small decrease and the SD of ζ slightly increased. This indicates that the residual citrate ions on AuNPs after $NaBH_4$ treatment were not prone to desorb.

X-ray Photoelectron Spectroscopy Characterization. Zeta potential data have shown that the changes in the zeta potential and interparticle interaction potentials were closely related to

AuNP charging via $NaBH_4$ treatment. It is possible that the citrate ions adsorbed on AuNPs were partially removed after the addition of $NaBH_4$ and that they readsorbed onto AuNPs after the discharge of injected electrons. The partial removal of citrate ions from the surfaces of AuNPs will result in a decrease in the surface potential of the AuNPs and eventually will induce a decrease in the total interaction potential.

To prove this hypothesis, XPS was used to examine the removal of adsorbed citrate ions on AuNPs before and after 6 mM $NaBH_4$ treatment (Figure 5). This study focused on C 1s and Au 4f spectral regions because these two elements are characteristic components of citrate-stabilized AuNPs. The XPS spectra of the C 1s core level were deconvolved into three separate peaks at 284.6, 286.2, and 288.2 eV that represent three different types of carbons: C−C/C−H, C−O, and COO^-, respectively.[36−38] For the substrate sample, two peaks appear at 284.6 and 288.2 eV but no peak is found at 288.2 eV (Figure 5a), which means that there was no COO^- component on the surface of the silicon substrate but there were C−O species. Therefore, the peaks appearing at 288.2 eV in Figure 5b−e should be due to the presence of citrate ions. Here, we used the peak area ratios of the three peaks to semiquantitatively analyze the change in the number of citrate ions on AuNPs before and after $NaBH_4$ treatment (Table 2). It is found that the content of COO^- from the citrate ions on AuNPs before purification is much higher than that after purification; this difference was also observed in the shape of the C 1s spectra (Figure 5b) and could be due to the residual excess amount of citrate in as-prepared AuNPs. However, the relative content of citrate ions on AuNPs decreased for the sample treated with 6 mM $NaBH_4$ for 10 min but increased again after 5 days, which was very similar to the change in the zeta potential. The obtained XPS data indicates that the decrease in the zeta potential after $NaBH_4$ treatment was due to the partial removal of citrate ions on AuNPs.

Table 2. Quantification of the Composition of C 1s of Concentrated AuNPs in Figure 5

	C 1s %		
sample	C−C	C−O	COO^- [a]
a	85.30	14.70	0
b	76.71	11.93	11.36
c	77.52	13.80	8.68 (100)
d	80.49	13.71	5.80 (67)
e	80.32	12.75	6.93 (80)

[a] The values in parentheses are the relative contents of citrate in samples c−e.

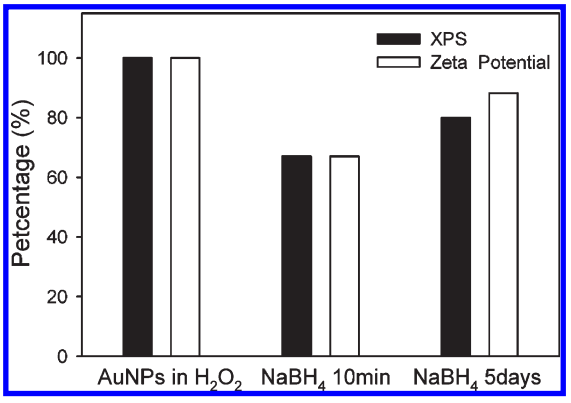

Figure 6. Comparison of the changing rates of the number of citrate ions on AuNPs after treatment with 6 mM $NaBH_4$ obtained by XPS and zeta potential measurements.

To compare the changing rates of citrate ions content after $NaBH_4$ treatment, the content of COO^- in sample c was used as the reference. The relative decreasing rate of change in citrate ions content in AuNPs after 10 min of $NaBH_4$ treatment was 33%, which agreed quite well with the decrease in the zeta potential measured in pure water (Figure 6). The XPS data also proved that excess $NaBH_4$ in solution did affect the zeta potential value measured 10 min after the addition of 6 mM $NaBH_4$. The restoration values of the number of citrate ions on AuNPs 5 days after $NaBH_4$ treatment were also similar, 80 and 88% respectively.

Figure 7 shows that no AuNP aggregates were formed by the addition of NaCl to pretreated $NaBH_4$ after 3 days or after the addition of H_2O_2, where the injected electrons had been greatly discharged from AuNPs. The restoration of citrate adsorption was further proven by this data.

Figure 5f shows the comparison of Au 4f spectra recorded before and after $NaBH_4$ treatment. The Au 4f peaks of AuNP without $NaBH_4$ treatment appear at 83.0 and 86.7 eV as a doublet corresponding to $4f_{7/2}$ and $4f_{5/2}$. The binding-energy separation of the two peaks is 3.7 eV, which is exactly the same as the standard separation of the Au^0 doublet ($4f_{7/2}$ and $4f_{5/2}$).[39] The doublet of Au 4f shifts toward higher binding energy after 6 mM $NaBH_4$ treatment (0.1 and 0.3 eV for 10 min and 5 days of treatment, respectively). It seems that the longer the $NaBH_4$ treatment takes, the more that the Au 4f peak is shifted. The sample of concentrated AuNPs (the same as sample D in Table 1) was used as a contrast. However, the shift of the Au 4f peak was 0.2 eV, which was intermediate between the two former samples. Also, the profile of C 1s spectra for this sample was nearly the same as that of sample d in Figure 5d (data not shown). This indicates that the shift of the Au 4f peak was strongly related to the time of reaction with H_2O after $NaBH_4$ treatment but not the excessive electron

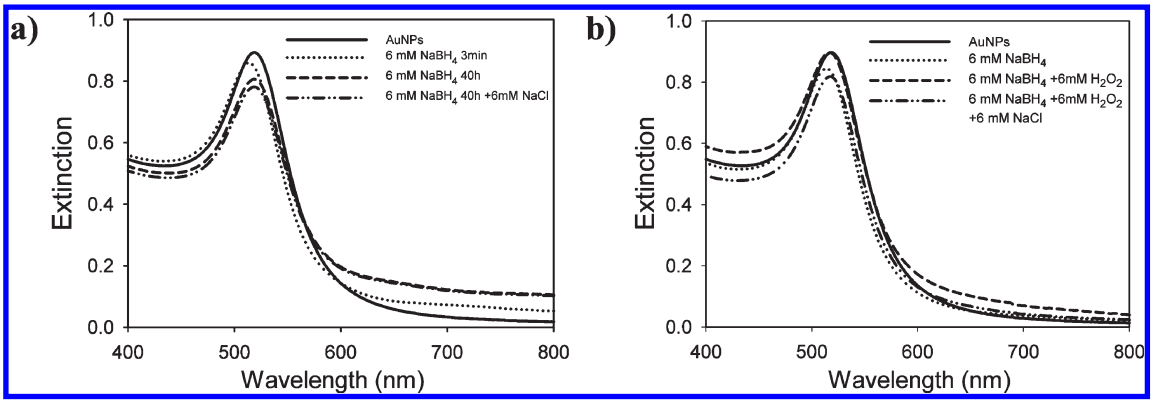

Figure 7. UV/vis extinction spectra of AuNPs after (a) slow discharge for 40 h and (b) rapid discharge through H_2O_2.

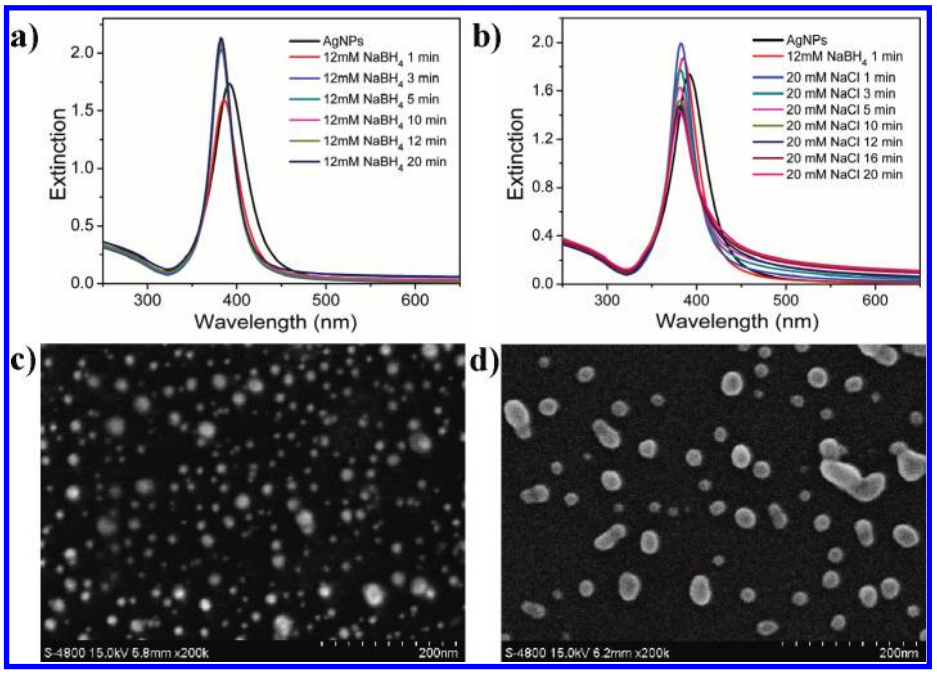

Figure 8. Temporal evolution of UV/vis extinction spectra of (a) silver nanoparticles treated with 12 mM $NaBH_4$ and (b) the addition of NaCl into an electron-injected Ag sol. (c, d) SEM images of a and b, respectively.

injection by $NaBH_4$. Moreover, the removal of citrate ions from the surfaces of AuNPs did not resulted from this significant shift in Au 4f because the citrate ions readsorbed onto the AuNPs, which showed a 0.3 eV shift in the binding energy. Here, we cannot clearly explain the shift in the Au 4f core-level binding energy after 5 days but we can at least conclude that the removal of citrate ions from the surfaces of AuNPs and the shift in the Au 4f binding energy resulted from the electron injection into AuNPs by $NaBH_4$.

We also tested the effect of $NaBH_4$ on the stability of citrate-stabilized AgNPs with λ_{max} at 392 nm. However, only the large blue shift of λ_{max} in the optical spectrum of the AgNP solution was observed after treatment with 12 mM $NaBH_4$, and SEM images shows no chainlike or network aggregates (Figure 8). Moreover, the addition of NaCl to the above solution induced a decrease in absorption at λ_{max} and an increase in the absorption band above 400 nm. The average size of AgNPs became about 2 times larger than the former, which was apparently induced by the coalescence of small AgNP aggregates. However, we found almost no change in the ζ value of AgNPs before and after 12 mM $NaBH_4$ treatment: they were -33.4 ± 19.6 and -32.7 ± 7.47 mV, respectively. Additionally, it was reported that citrate ions remained on the AgNPs after $NaBH_4$ treatment, which was characterized by surface-enhanced Raman scattering (SERS).[40] These data indicated that injected electrons have no notable effect on the decrease in Ψ_0. This distinct difference between AuNPs and AgNPs may due to the different types of carboxylate coordination with the two noble metals.

Mechanism of $NaBH_4$-Induced Aggregation of AuNPs. To understand the aggregation of AuNPs, we must quantify the interaction potential between NPs according to DLVO theory.

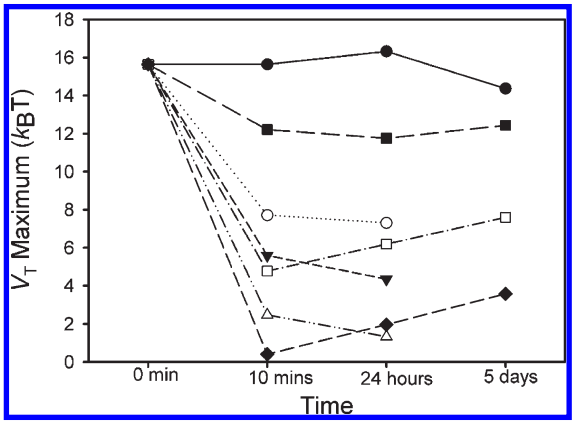

Figure 9. Calculated total interaction potential maximum when treated with various concentrations of NaCl [(●) 0, (○) 3, (▼) 6, and (△) 12 mM] and $NaBH_4$ [(■) 0.4, (□) 3, and (♦) 6 mM]. The ionic strength of the as-prepared AuNP dispersion (about 2 mM) is involved in the calculation.

According to eqs 2−5, V_{elec} is related to the surface potential (Ψ_0) and the ionic strength of the solution. Ψ_0 cannot be determined directly by experiment, but it can be partially reflected in the zeta potential of AuNPs, which is the potential at the surface of shear and is definitely less than the potential at the surface Ψ_0.[25] For a crude calculation, we assume that the Ψ_0 values are 1.5 times larger than the ζ values (Table 1); the total interaction potential maximum (V_{tmax}) after the addition of different amounts of NaCl and $NaBH_4$ is shown in Figure 9. The calculation shows that V_{tmax} decreased significantly after the addition of $NaBH_4$ and increased again within 5 days. This restoration of V_{tmax} indicates that the AuNPs will become stable again after the discharge of the AuNPs, which agrees well with the stability of the optical spectra after 24 h. It also should be noticed that the ζ values induced by 3 and 6 mM $NaBH_4$ are almost equal, which means that 3 mM $NaBH_4$ is enough to reduce ζ and that more $NaBH_4$ added to the AuNP solution just decreases the velocity of restoring the ζ. Accordingly, the calculated V_{tmax} induced by 3 mM $NaBH_4$ is

(36) Puniredd, S. R.; Srinivasan, M. P. *Langmuir* **2006**, *22*, 4092.
(37) Inagaki, N. *Plasma Surface Modification and Plasma Polymerization*; Technomic: Lancaster, PA, 1996; p 26.
(38) Yoshida, Y.; Van Meerbeek, B.; Nakayama, Y.; Snauwaert, J.; Hellemans, L.; Lambrechts, P.; Vanherle, G.; Wakasa, K. *J. Dent. Res.* **2003**, *82*, 136.
(39) Brust, M.; Walker, M.; Bethell, D.; Schiffrin, D. J.; Whyman, R. *J. Chem. Soc., Chem. Commun.* **1994**, 801.
(40) Blatchford, C. G.; Sllman, O.; Kerker, M. *J. Phys. Chem.* **1983**, *87*, 2503.

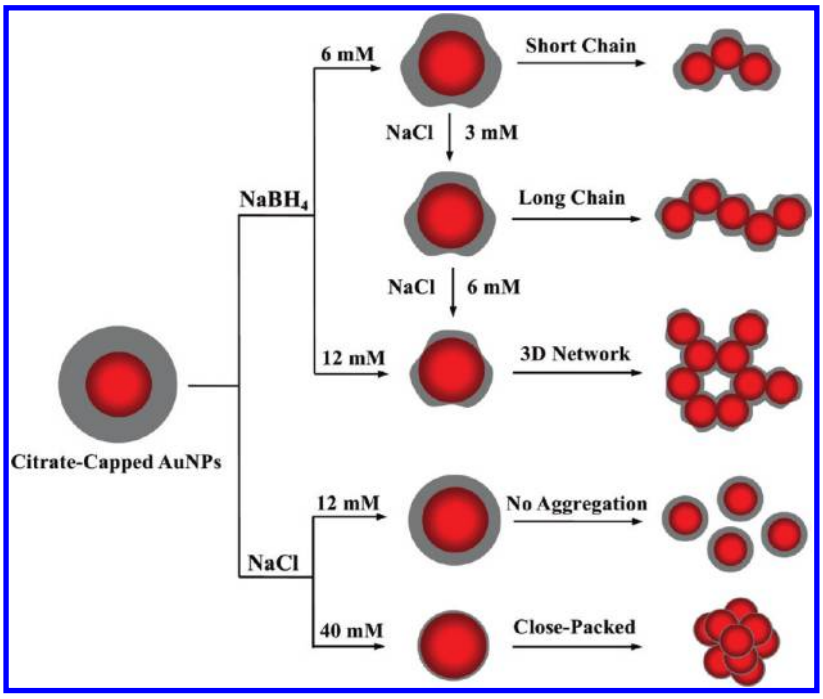

Figure 10. Possible mechanism of the aggregation of irregular chainlike aggregates and 3D network aggregates of Au nanoparticles based on the concentrations of $NaBH_4$ and NaCl. The decreased isotropic electrostatic repulsion caused by NaCl could not induce anisotropic aggregates.

much higher than that induced by 6 mM $NaBH_4$, which indicates that $NaBH_4$-treated AuNPs are sensitive to ionic strength. It also indicates that the controlled aggregation of AuNPs (Figure 2), in fact, was induced by the increase in the ionic strength.

Previous studies[41] have suggested that most solution-phase strategies for the synthesis of metallic NPs (gold and silver) are a mixture of various morphologies such as decahedrons, tetrahedrons, truncated tetrahedrons, and cubes. Colloidal gold (silver) is also usually composed of single-crystalline, singly twinned, and multiply twinned structures. These nonideal spherical NPs have different crystalline facets with different chemical activities.[42] In this sense, the strength of the binding force of the stabilizer on different crystalline facets of NPs is not uniform. As a result, the stabilizers with a weak binding force on some facets will desorb first under the same treatment. It has been reported that citrate ions could adsorb and form stable, well-ordered adlayers on the gold surface through surface coordination.[43] The coordination of deprotonated carboxylate groups with gold may be disturbed by $NaBH_4$ treatment. Consequently, some citrate ions with a low binding affinity to AuNPs were removed first and an anisotropic distribution of surface charge formed. The anisotropy of the surface charge distribution transforms isotropic electrostatic repulsion between AuNPs into anisotropic forms (Figure 10). It is worth noting that the addition of $NaBH_4$ to the sol also increases the ionic strength. Such dual roles of $NaBH_4$ provide a rapid decrease in electrostatic repulsion. By increasing the ionic strength using NaCl after 6 mM $NaBH_4$ treatment, a slow reduction of electrostatic repulsion can be obtained, which is more suitable for finely controlling aggregation. The irregular chainlike aggregates and 3D network aggregates of AuNPs are formed by controlling the strength of the anisotropic electrostatic repulsion. Importantly, the redistribution of surface charges after a few NPs are assembled plays an important role in anisotropic self-assembly. The growth of irregular chainlike aggregates can be explained by the electrostatic interaction model,[44] where the length of the chain increases with the reduction of electrostatic repulsion. When the strength of the electrostatic repulsion was greatly decreased by $NaBH_4$ treatment and the ionic strength, the assembly of NPs provided less repulsion and 3D porous aggregates were formed in the final stage.

Conclusions

Treating the citrate-stabilized AuNP solutions with various amounts of $NaBH_4$ induced a blue shift in the surface plasmon resonance peak (λ_{max}) and caused a different extent of AuNP aggregation. By increasing the ionic strength of AuNP solutions after treatment with a lower concentration of $NaBH_4$, non-close-packed aggregates including irregular chainlike aggregates and 3D network aggregates of AuNPs can be obtained. Zeta potential and XPS characterization showed that citrate ions on AuNPs were partially removed from the surfaces of AuNPs after the addition of $NaBH_4$. The partial removal of citrate ions produces an anisotropic charge distribution around the AuNPs and eventually transforms the isotropic electrostatic repulsion between the NPs into an anisotropic one. This is quite different from previous methods[9−12] in which the citrate ions were replaced with other chemicals. The aggregates that formed in solution are stable because citrate ions readsorbed on AuNPs after discharge. Additionally, the non-close-packed aggregates of AuNPs formed by $NaBH_4$ treatment, which are in an activated state and do not involve surfactant chemicals, could be used in areas such as photonics, electrocatalysis, and SERS.

Acknowledgment. We thank the National Natural Science Foundation of China (no. 60971025), the National High-Tech

(41) (a) Wiley, B.; Herricks, T.; Sun, Y.; Xia, Y. *Nano Lett.* **2004**, *4*, 1733. (b) Wiley, B.; Sun, Y.; Chen, J.; Cang, H.; Li, Z.-Y.; Li, X.; Xia, Y. *MRS Bull.* **2005**, *30*, 356.
(42) (a) Xia, Y.; Xiong, Y.; Lim, B.; Skrabalak, S. E. *Angew. Chem., Int. Ed.* **2008**, *47*, 2. (b) Tao, A. R.; Habas, S.; Yang, P. *Small* **2008**, *4*, 310.
(43) Lin, Y.; Pan, G.-B.; Su, G.-J.; Fang, X.-H.; Wan, L.-J.; Bai, C.-L. *Langmuir* **2003**, *19*, 10000.
(44) Zhang, H.; Yang, D. *Angew. Chem., Int. Ed.* **2008**, *47*, 3984.

Research and Development Program of China (no. 2006AA040367), and the Knowledge Innovation Programs of the Chinese Academy of Sciences (no. KJCX2-YW-H18) for financial support.

Supporting Information Available: UV/vis extinction spectra of citrate-stabilized AuNPs (particle size 17 nm) recorded 1 h after the addition of $NaBH_4$, AuNPs pretreated with 6 mM $NaBH_4$ after the addition of different amounts of NaCl within 3 days, and AuNP solutions pretreated with 6 mM $NaBH_4$ after the addition of NaF and NaOH. pH of AuNP solutions after the addition of various amounts of $NaBH_4$ within 5 days. Zeta potential of AuNP solutions with pH ranging from 5.2 to 10.0. This material is available free of charge via the Internet at http://pubs.acs.org.